Chapter 2
Rotational and Translational Diffusion in Ionic Liquids

Joshua Sangoro, Tyler Cosby and Friedrich Kremer

Abstract Dynamic glass transition and charge transport in a variety of glass-forming aprotic ionic liquids (ILs) are investigated in wide frequency and temperature ranges by means of broadband dielectric spectroscopy (BDS), pulsed-field gradient nuclear magnetic resonance (PFG NMR), differential scanning calorimetry and dynamic mechanical spectroscopy. On the low-frequency side, the dielectric spectra exhibit electrode polarization effects, while hopping conduction in a disordered matrix dominates the spectra of ionic liquids at higher frequencies. Upon systematic variation of the molecular structure of the ionic liquids, it is observed that the absolute values of dc conductivity and viscosity span more than 11 orders of magnitude with temperature. However, quantitative agreement is found between the characteristic charge transport and the structural α-relaxation rates. These results are discussed in the context of *dynamic glass transition-assisted hopping* as the underlying mechanism of charge transport in the ionic liquids investigated. In addition, a novel approach to determine diffusion coefficients from dielectric spectra in quantitative agreement with PFG NMR is proposed. This makes it possible to separately determine the effective number densities and mobilities of the charge carriers and the type of their temperature dependence. The observed Vogel–Fulcher–Tammann (VFT) dependence of the dc conductivity is shown to be due to a similar temperature dependence of the mobility while Arrhenius type of thermal activation is found for the number density.

J. Sangoro (✉) · T. Cosby
Department of Chemical and Biomolecular Engineering, University of Tennessee,
1512 Middle Drive, Knoxville, TN 37932, USA
e-mail: jsangoro@utk.edu

T. Cosby
e-mail: jcosby3@vols.utk.edu

F. Kremer
Institute of Experimental Physics I, University of Leipzig, Linnestr. 5,
04103 Leipzig, Germany
e-mail: kremer@physik.uni-leipzig.de

M. Paluch (ed.), *Dielectric Properties of Ionic Liquids*,
Advances in Dielectrics, DOI 10.1007/978-3-319-32489-0_2

Keywords Ionic liquids · Diffusion · Charge transport rate · DC conductivity · Einstein–Smoluchowski relations · Green–Kubo relations · Effective number density · Random barrier model

2.1 Introduction

Fruitful and exciting periods of scientific and technological research often ensue the discovery of a novel material. As succinctly stated by Yves Chauvin in his 2005 Nobel address: "*If you want to find something new, look for something new!*" [1]. New breakthroughs offer possibilities to critically re-examine old problems as well as to pose new ones. This is the case with ionic liquids, liquids consisting entirely of cations and anions with melting points below 100 °C. Ionic liquids are interesting for both fundamental as well as technological applications. Depending on the composition and chemical characteristics of the constituent molecular moieties comprising the ionic liquids, they may be classified into two main categories, namely aprotic and protic ionic liquids. This chapter focuses on studies of aprotic ionic liquids. Although no single ionic liquid possesses all these characteristics, aprotic ionic liquids in general show a rich mix of outstanding properties such as low melting temperatures, high ionic conductivity, negligible vapour pressures, wide liquidus ranges, high thermal and electrochemical stability and tunability. Despite reports dating back to Paul Walden's work in 1914 [2, 3], there has been a heightened interest in ionic liquids during the last two decades due to their unique properties which make them especially attractive for use in reaction media, as electrolytes in electrochemical energy technologies, among many others. Some of the significant areas of applications of ionic liquids are illustrated in Fig. 2.1.

From a fundamental point of view, the fact that ionic liquids can be easily supercooled makes them interesting materials to use as platforms for investigating the interplay between the dynamic glass transition and charge transport in amorphous liquids. In a sense, this involves re-examination of basic relations put forward by Einstein [4], Smoluchowski [5, 6], Maxwell [7, 8], Langevin [9] and Debye [10] concerning rotational and translational diffusion in (conducting) liquids. Although the different terminologies are employed today, certain aspects of the topics addressed by these scientists still remain unsolved. For instance, there is no general quantitative theory of dynamic glass transition (treated by Debye as rotational Brownian motion based on Einstein's ideas) which is able to reproduce all the observed experimental results to date, notwithstanding the significant advances achieved so far from experimental and theoretical studies. Another outstanding example is Einstein's work on Brownian motion in which he derived the link between translational diffusion (or charge transport) and viscosity (related to rotational diffusion). One of the objectives of the current chapter is to verify how well these classical relations hold in glass-forming ionic liquids.

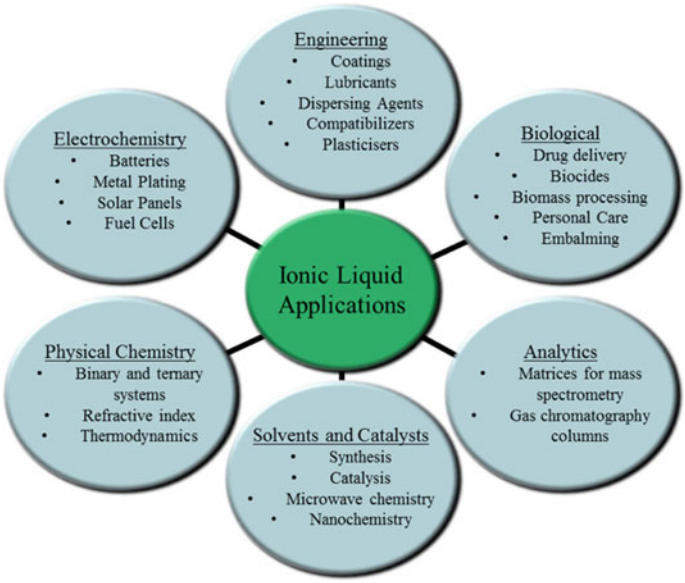

Fig. 2.1 Some possible applications of ionic liquids

Since it measures the complex dielectric function (and consequently, the complex conductivity) over many orders of magnitude in frequency and in a wide temperature interval, broadband dielectric spectroscopy (BDS) has proved to be an ideal experimental tool for addressing basic questions regarding the correlation between ion conduction (translational diffusion) and the dynamic glass transition (rotational diffusion) in broad length- and timescales as well as localized molecular fluctuations (secondary relaxations) [11–32]. Detailed knowledge of diffusion in ionic liquids, provided by this technique, is instructive for their optimal utilization in a wide range of scientific and technological applications.

It is estimated that it may be possible to synthesize approximately 10^{18} different ionic liquids based on the combinations of cations and anions available [20, 33]. This high degree of tunability has its challenges as well. Use of a trial-and-error approach in the synthesis of ionic liquids in search of one exhibiting particular physical and chemical properties is therefore not viable. Thus, it is imperative that more general relationships between the desirable properties such as high conductivities and the nature as well as structure of anions and cations be established. Molecular dynamics simulations are being conducted to make quantitative predictions of the physical properties of ionic liquids. In this chapter, it is shown that characteristic hopping lengths (determined from a combination of broadband dielectric spectroscopy and pulsed-field gradient nuclear magnetic resonance) in a selected series of ionic liquids increase with the molecular volume obtained from quantum chemical simulations.

2.2 Experimental Details

The ionic liquids investigated in this study (1-hexyl-3-methylimidazolium chloride—[HMIM] [Cl], 1-hexyl-3-methylimidazolium bromide—[HMIM] [Br], 1-hexyl-3-methylimidazolium iodide—[HMIM] [I], 1-hexyl-3-methylimidazolium tetrafluoroborate—[HMIM] [BF4], 1-hexyl-3-methylimidazolium hexafluorophosphate—[HMIM] [PF6], 1-(2-hydroxyethyl)-3-methylimidazolium tetrafluoroborate—[HEMIM] [BF4], 1-methyl-3-octylimidazolium tetrafluoroborate—[MOIM] [BF4], 1-butyl-3-methylimidazolium tetrafluoroborate—[BMIM] [BF4], 1,3-dimethylimidazolium dimethylphosphate—[MMIM] [Me2PO4], 1-ethyl-3-methyl-pyridinium ethylsulfate—[3-MEP] [EtSO4], Trioctylmethylammonium bis (trifluoromethylsulfonyl)imide—[OMA] [BTA] and Tetrabutylphosphonium bromide—[TBP] [Br]) were purchased from Solvent Innovation GmbH and Iolitec GmbH. Tributyloctylphosphonium trifluoromethanesulfonate—[TBOP] [OTf] was provided by Prof. Dr. Katsuhiko Tsunashima, National Institute of Technology, Wakayama College. (1-propyl-3-methylimidazolium bis(trifluoromethylsulfonyl) imide—[PrMIM] [NTf2], 1-butyl-3-methylimidazolium bis(trifluoromethylsulfonyl)imide—[BMIM] [NTf2], 1-hexyl-3-methylimidazolium bis(trifluoromethylsulfonyl)imide—[HMIM] [NTf2], 1-octyl-3-methylimidazolium bis(trifluoromethylsulfonyl)imide—[OMIM] [NTf2], 1-decyl-3-methylimidazolium bis(trifluoromethylsulfonyl)imide—[DMIM] [NTf2], 1-pentyl-3-vinylimidazolium bis (trifluoromethylsulfonyl)—[PVIM] [NTf2], 1-octyl-3-vinylimidazolium bis (trifluoromethylsulfonyl)—[OVIM] [NTf2]) were prepared by Prof. Dr. Veronika Strehmel, Hochschule Niederrhein University of Applied Sciences. The chemical structures of the cations and anions investigated are shown in Tables 2.1 and 2.2, respectively. The dielectric measurements were performed between 0.01 Hz and 1.8 GHz using a novocontrol high-resolution alpha analyzer (0.01 Hz–10 MHz) and an HP impedance analyzer (1 MHz–1.8 GHz). The analyzers were assisted by Quatro Temperature Controllers using pure nitrogen as heating agent and assuring a temperature stability better than 0.2 K. An ARES (Advanced Rheometric Expansion System) rheometer from TA Instruments was employed for Dynamic Mechanical Spectroscopy (DMS) measurements. A 400 MHz NMR spectrometer with a home-built gradient device was used to obtain the self-diffusivities at different temperatures.

2.3 Results and Discussion

In this chapter, the dielectric properties of ionic liquids are investigated in broad frequency and temperature ranges. Emphasis is placed on quantitative understanding of the underlying mechanisms as well as the interplay between charge transport and glassy dynamics in these materials. Quantum chemical calculations of molecular volumes of ionic liquids are performed using MOPAC2009 package in

Table 2.1 Chemical structures of typical cations in ionic liquids

1 - alkyl - 3-methylimidazolium	Tetra-alkyl-ammonium
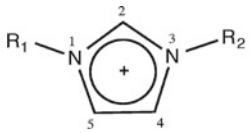	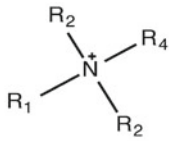
Tetra-alkyl-phosphonium	N-alkyl-pyridinium
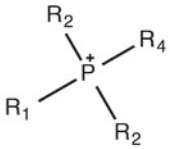	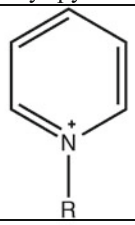
N-alkyl-N-methylpiperidinium	Symbol key
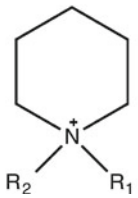	$R_{1,2,3,4}$= $CH_3(CH_2)_n$, (n = 1,3,5,7,9), aryl, etc...

order to re-examine the predictions of Einstein concerning the dependence of the diffusion coefficient on molecular sizes. The following techniques are employed: broadband dielectric spectroscopy, pulsed-field gradient nuclear magnetic resonance, differential scanning calorimetry and dynamic mechanical spectroscopy.

2.3.1 Charge Transport and Dynamic Glass Transition in Ionic Liquids

Broadband dielectric spectroscopy (BDS) measures the complex dielectric function, ε^*, which is equivalent to the complex conductivity function, σ^*. This is expressed as

Table 2.2 Chemical structures of some of the anions comprising the ionic liquids investigated

$[BF_4]^-$	$[Me_2PO_4]^-$
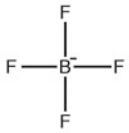	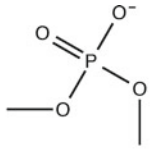
$[NTf_2]^-$	[ethyl sulfate]$^-$
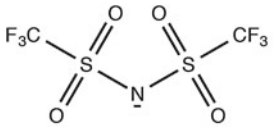	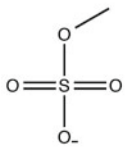
$[OTf]^-$	$[PF_6]^-$
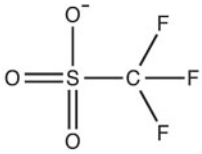	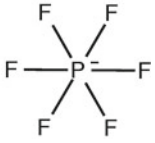
$[NO_3]^-$	[halides]$^-$
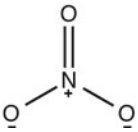	Cl^-, Br^-, I^-

$\sigma^*(\omega, T) = i\varepsilon_0\omega\varepsilon^*(\omega, T)$, implying that $\sigma' = \varepsilon_0\omega\varepsilon''$ and $\sigma'' = \varepsilon_0\omega\varepsilon'$ (ε_0 being the vacuum permittivity and ω the radial frequency) [32]. The dielectric spectra of the ionic liquid [HMIM] [Cl] are presented in Fig. 2.2. The real part of the complex conductivity σ' is characterized on the low-frequency side by a plateau (the value of which directly yields the long range ionic conductivity, σ_0), and the characteristic rate, ω_c, at which dispersion sets in and turns into a power law at higher frequencies. On the other hand, the real part of the complex dielectric function ε' turns from the high frequency limit to the static value ε_s at the characteristic rate ω_c. At lower frequencies, it is observed that σ' decreases from σ_0 value and this is due to electrode polarization that results from slowing down of charge carriers at the electrodes.

Rescaled with respect to ω_c and σ_0, the dielectric spectra—as measured over wide temperature ranges—coincide (see Fig. 2.3), thus proving the uniqueness of

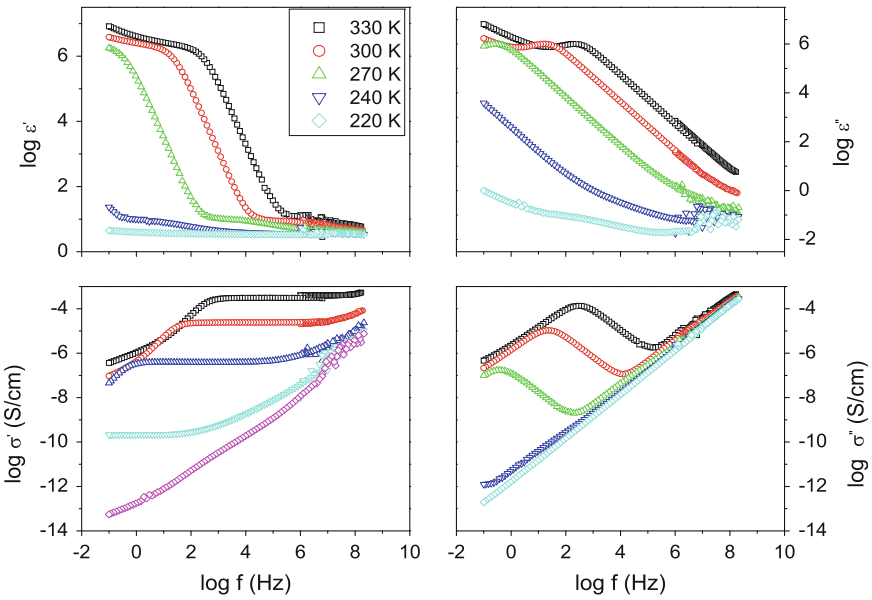

Fig. 2.2 Complex dielectric function $(\varepsilon^* = \varepsilon' - i\varepsilon'')$ and complex conductivity function $(\sigma^* = \sigma' + i\sigma'')$ of the ionic liquid 1-hexyl-3-methylimidazolium chloride—[HMIM] [Cl] at different temperatures as indicated. The error bars are comparable to the size of the symbols, if not explicitly indicated otherwise. The logarithm is to base 10

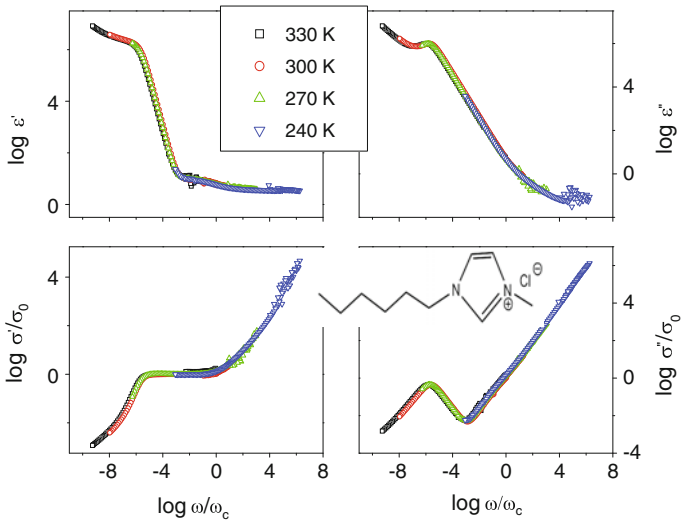

Fig. 2.3 Scaling of the complex dielectric function $(\varepsilon^* = \varepsilon' - i\varepsilon'')$ and complex conductivity function $(\sigma^* = \sigma' + i\sigma'')$ with respect to ω_c and σ_0 for the ionic liquid 1-hexyl-3-methylimidazolium chloride—[HMIM] [Cl] at different temperatures

the mechanism of charge transport. It can be concluded that the underlying processes in the spectral and temperature ranges probed exhibit identical thermal activation [22, 23, 34–36].

Charge transport in many amorphous ion-conducting systems is reasonably well described by random barrier model developed by Dyre [37]. In the context of this model, ions hop in a random spatially distributed potential landscape. The ion transport is determined by the ability of the charge carriers to hop over the random energy barriers. The success of the ions in surmounting the highest barrier determines long range or dc conductivity σ_0 [38]. The time corresponding to the attempt rate to overcome the highest barrier is denoted by τ_e. The analytical solution for the complex dielectric function, obtained within the continuous-time-random walk approximation, is expressed as

$$\varepsilon^*(\omega) = \frac{\sigma_0 \tau_e}{\varepsilon_0 \ln(1 + i\omega\tau_e).} \tag{2.1}$$

It has been demonstrated that the approximate form of the random barrier model given in Eq. 2.1 describes the dielectric spectra of many different ion-conducting systems qualitatively well. However, a close examination of the fits of the dielectric spectra of ionic liquids reveals the existence of additional 'relaxation-like' process. This contribution is particularly dominant in the real part of the complex dielectric function. Apparently, this additional process was neglected in many earlier dielectric studies of ionic liquids but its possible origin is fairly obvious. From a physical point of view, a successful ionic jump must be accompanied by structural reorganization of the ionic atmosphere, leading to a relaxation-like contribution not only to the imaginary part, but also to the real part of the dielectric function. This reorganization accompanying successful ion jumps causes additional fluctuations in the polarization, resulting in a relaxation process with characteristic timescales similar to that of ionic motion.

From the definition of polarization **P** in terms of the complex dielectric function $\varepsilon^*(\omega)$, Debye employed the Lorentz field and substituted the static permittivity with the dynamic permittivity obtaining

$$\mathbf{P} = \varepsilon_0(\varepsilon^*(\omega) - 1)\mathbf{E} = N_1\left[\alpha_\infty + \frac{\mu^2}{3kT(1 + i\omega\tau_D)}\right]\frac{\varepsilon^*(\omega) + 2}{3}\mathbf{E} \tag{2.2}$$

where α_∞ and N_1 denote the polarizability and number of dipoles per unit volume, respectively, and τ_D is the Debye macroscopic relaxation time. Defining ε_s and ε_∞ as the unrelaxed and relaxed values of the dielectric permittivity, respectively, Eq. 2.2 can be rearranged as

$$\frac{\varepsilon^*(\omega) - \varepsilon_\infty}{\varepsilon_s - \varepsilon_\infty} = \frac{1}{1 + i\omega\tau_D} \tag{2.3}$$

The Debye equations of dielectric permittivity can also be derived by considering the first-order kinetics of rise or decay of the dipolar polarization. Further details can be found in [32, 39].

It should be recalled that although the Debye theory of dielectric relaxation resulted from rigorous treatment of rotational Brownian motion, Debye-like relaxations are only observed in rare cases in glass-forming systems. The usual dielectric spectra are much broader than predicted by Debye's approach. Thus, a number of phenomenological descriptions aimed at obtaining better fits to experimental data like the Cole-Cole, Cole–Davidson and Havriliak–Negami functions have been proposed. The empirical Havriliak–Negami function is the most commonly used form to fit the spectra of many materials exhibiting dielectric relaxations. Within this approach, the complex dielectric function is given by

$$\varepsilon^*_{\mathrm{HN}} = \varepsilon_\infty + \frac{\Delta\varepsilon}{\left(1 + (i\omega\tau_{\mathrm{HN}})^\beta\right)^\gamma} \tag{2.4}$$

where $\Delta\varepsilon = \varepsilon_s - \varepsilon_\infty$ is the dielectric relaxation strength or intensity with $\varepsilon_s = \lim_{\omega\tau_{\mathrm{HN}} \geq 1} \varepsilon'(\omega)$ and $\varepsilon_\infty = \lim_{\omega\tau_{\mathrm{HN}} \leq 1} \varepsilon'(\omega)$. The shape parameters β and γ describe symmetric and asymmetric broadening of the complex dielectric function. The position of maximal loss ω_{p} depends on the characteristic time obtained from Eq. 2.4 as well as the shape parameters according to $\omega_{\mathrm{p}} = \frac{1}{\tau_{\mathrm{HN}}}\left[\sin\frac{\beta\pi}{2+2\gamma}\right]^{\frac{1}{\beta}}\left[\sin\frac{\beta\gamma\pi}{2+2\gamma}\right]^{-\frac{1}{\beta}}$. It should be noted that the real and imaginary parts of the complex dielectric function are related by the Kramers–Kronig relations [32, 40].

Thus, to account for ionic motion and the accompanying structural reorganization, the complex dielectric function should be described by Eq. 2.5:

$$\varepsilon^*(\omega) = \frac{\sigma_0\tau_{\mathrm{e}}}{\varepsilon_0 \ln(1 + i\omega\tau_{\mathrm{e}})} + \frac{\Delta\varepsilon}{\left(1 + (i\omega\tau_{\mathrm{HN}})^\beta\right)^\gamma} + \varepsilon_\infty \tag{2.5}$$

where ε_∞ is the (high frequency) relaxed value of ε'. As shown in Fig. 2.4 for [TBOP] [OTf], Eq. 2.5 yields a quantitative fit to the part of the experimental spectra dominated by charge transport.

The dielectric spectra of ionic disordered materials can also be presented in terms of the electrical modulus M^*, where $M^* = 1/\varepsilon^*$. Although the three formalisms (complex dielectric, conductivity and modulus functions) are equivalent, they emphasize different aspects of the underlying mechanisms of charge transport and molecular dynamics. The first two forms—the complex dielectric and conductivity functions—have traditionally been used in studies of (dipolar) relaxations and charge transport, respectively. Maxwell's equations, which describe the interaction of electromagnetic waves with matter, make direct reference to and indicate equivalence of these approaches. At higher frequencies, secondary relaxations

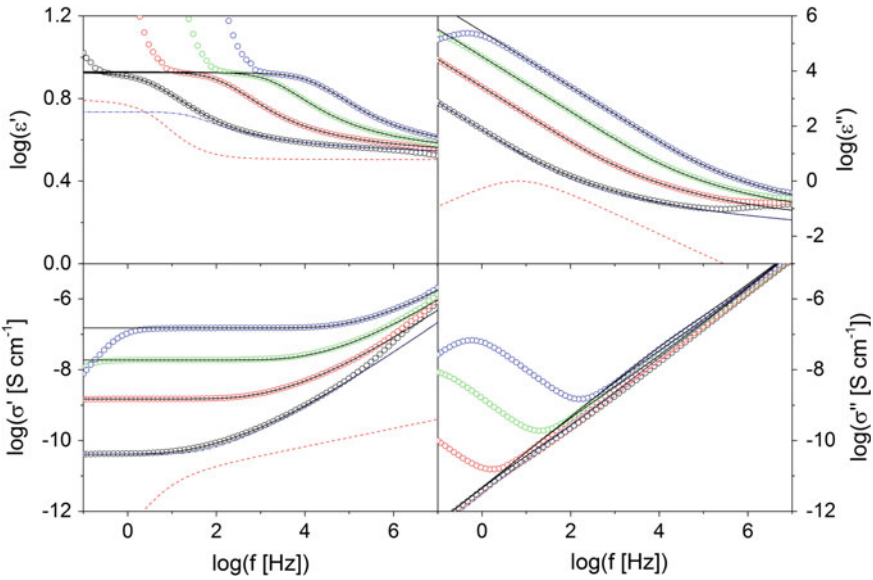

Fig. 2.4 The dielectric and conductivity functions for [TBOP] [OTf] versus frequency at different temperatures, as indicated. The fits are made using Eq. 2.5. The spectra are shown at temperatures from 210 to 240 K (10 K increments). The *continuous solid lines* denote the combination of the Havriliak–Negami (*red*) and random barrier model (*blue*) functions. The error bars are comparable to the size of the symbols, if not specified otherwise

(denoted by rate ω_β) are observed. We recently showed that these dipolar processes are due to librations of the cations [23, 41].

In the intermediate frequency ranges, the dielectric properties are governed by motion of the charge carriers in the bulk. This contribution represents the (translational) diffusion of the ions. This regime of the dielectric spectra can be used to obtain important molecular parameters characterizing translational diffusion of the charge carriers. Electrode polarization dominates the spectra at lower frequencies.

Empirically, $\omega_c \cong \omega_M \cong 1/\tau_e$ as shown in Fig. 2.5, where ω_M is the radial frequency corresponding to the peak in the imaginary part of the electrical modulus and $\omega_e = (1/\tau_e)$ is a characteristic time that defines the attempt rate of the charge carriers to overcome the highest energy barrier (limiting the σ_0), thereby enabling the physical interpretation of ω_c within the random barrier model [32, 37].

To find out the impact of molecular structure and composition on charge transport and dynamics of these systems, ionic liquids based on the HMIM cation are systematically investigated upon variation of the anions. The thermal activation of σ_0 and ω_c—the central quantities describing ion transport—are studied. It is clear that systematic changes of the anions while keeping the same [HMIM] cation result in substantial differences in the charge transport parameters. These differences become more significant as the temperature is lowered towards the calorimetric glass transition temperature of the ionic liquid under study. In order to find out the

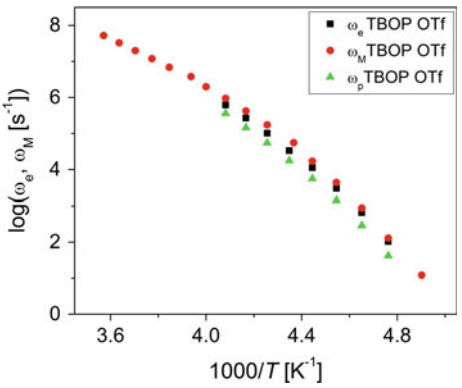

Fig. 2.5 Activation plot for characteristic electrical rates ω_M (as obtained from the peak frequency of M''), ω_e and ω_p as taken from the fit using Eq. 2.5 for TBOP OTf. The error bars are smaller than the size of the symbols, if not explicitly stated otherwise. The logarithm is to base 10

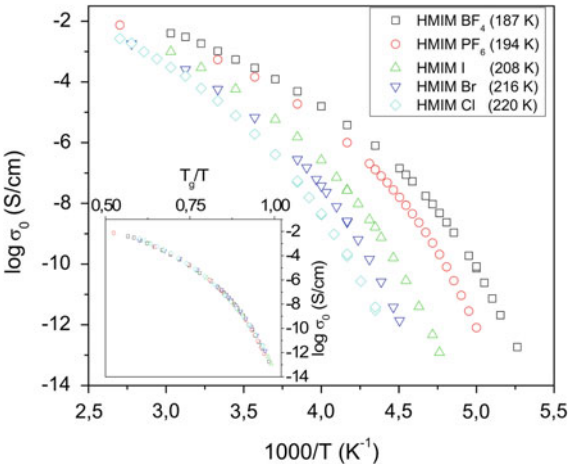

Fig. 2.6 Temperature dependence of σ_0 (T) for the selected ionic liquids is shown. *Inset* Scaling with respect to the calorimetric glass transition temperature (values given in the legend) determined by differential scanning calorimetry. Reproduced from Ref. [34] with permission from the PCCP Owner Societies

impact of the dynamic glass transition on charge transport in ionic liquids, dc conductivity and viscosity measurements were performed for a systematic series of ionic liquids, upon variation of the anions. Figure 2.6 presents the temperature dependence of σ_0 for the selected ionic liquids.

Systematic variation of the chemical structure leads to remarkable differences exceeding six orders of magnitude in σ_0 (between the tetrafluoroborate and chloride anions) at lower temperatures. However, upon scaling with the calorimetric glass transition temperature, all the data coincide for the anions examined. This experimental finding highlights the important role played by dynamic glass transition in charge transport in ionic liquids. In addition, viscosity, η,—well known to be directly related to the dynamic glass transition in liquids—also exhibits a similar thermal activation. The significant changes in the viscosity and ω_c upon systematic variation of the anions is also worth pointing out as presented in Fig. 2.7.

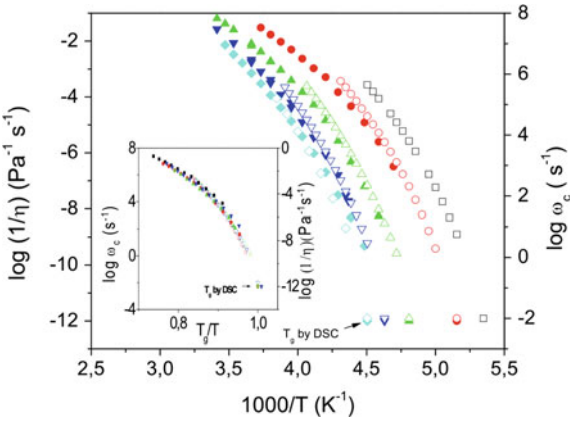

Fig. 2.7 Thermal activation of the fluidity (inverse viscosity) 1/η (*T*) and ω_e (*T*) for the series of imidazolium-based ionic liquids upon variation of the anions. *Inset* Scaling with respect to the calorimetric glass transition temperature obtained by differential scanning calorimetry (see legend of Fig. 2.6). The symbols are identical to those in Fig. 2.6 with 1/η (*T*) and ω_c (*T*) represented by *full* and *open symbols*, respectively. Reproduced from Ref. [34] with permission from the PCCP Owner Societies

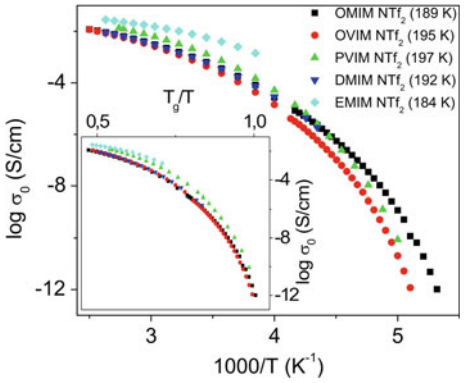

Fig. 2.8 Temperature dependence of $\sigma_0(T)$. *Inset* Scaling with respect to the calorimetric glass transition temperature (as shown) measured by differential scanning calorimetry) for selected bis (trifluoromethylsulfonyl) imide-based ionic liquids

Extrapolating ω_c to the timescale corresponding to 100 s, agreement with the measured calorimetric glass transition temperature T_g within margins of ±2 K is found. Scaling of σ_0 (*T*), ω_c (*T*), and 1/η(*T*) with respect to T_g using the approach proposed by Angell [42–45], coinciding plots for all the investigated ionic liquids are found as shown in Figs. 2.6 and 2.7. On the other hand, upon varying the cation and maintaining the same anion, deviations can be observed in the scaled plot of σ_0 (*T*). This is illustrated for the bis(trifluoromethylsulfonyl)imide-based ionic liquids in Fig. 2.8. Our conjecture is that the since the size of the cation in ionic liquids is larger than that of the anion, the cations play a more pronounced role in determining the viscosity and structural relaxation (and consequently charge transport). It should be

recalled that electrostatic interactions, which control the dynamic glass transition in these materials, are strongly influenced by both the charge as well as the distance of separation between the interacting ions.

Using the Einstein and Einstein–Smoluchowski equations together with the definition of dc conductivity, one obtains [23, 34]:

$$\sigma_0(T) = q\mu(T)n(T) = n(T)\frac{q^2 D(T)}{kT} = n(T)\frac{q^2\lambda^2\omega_c(T)}{6kT} \tag{2.6}$$

where n denotes the effective number density of charge carriers contributing to ion transport at the timescale of ω_c, λ refers to the characteristic diffusion length in this timescale, also taken characterizing the cross-over from non-random diffusion to random diffusion [46], D is the diffusion coefficient, μ is the mobility, q is the elementary charge and k denotes the Boltzmann constant. Therefore, $\sigma_0 \propto \omega_c$ as implied by the empirical BNN relation and in full agreement with the results presented in Fig. 2.9. It is noteworthy that the data coincide for all the ionic liquids investigated despite variations of the absolute values of both the dc conductivity and the characteristic rates spanning more than 11 decades upon changes in the temperature, pressure as well as composition.

In his paper on Brownian motion, Einstein [4] derived the first form of what is currently known as the fluctuation—dissipation theorem, linking position fluctuations to a dissipation (viscosity). This relation forms the basis of the linear response theory emphasized by Kubo [47] and is of direct relevance in the current studies. Einstein showed that

$$\left\langle x^2 \right\rangle_t = 2Dt = \frac{RT}{N}\frac{t}{3\pi\eta a} \tag{2.7}$$

where $\left\langle x^2 \right\rangle_t$ denote the position fluctuations (completely identical to λ^2 employed in Eq. 2.6), t is a measure of the timescale (equivalent to $1/\omega_c$ in the current work), R the gas constant, N the Avogadro number and a the Stoke's radius. Upon

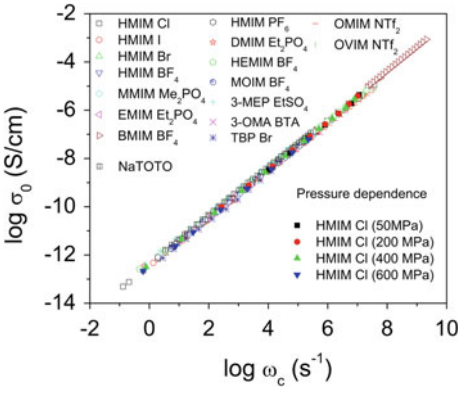

Fig. 2.9 The dc conductivity, σ_0, versus the characteristic charge transport rate, ω_c, for different ionic liquids as indicated. The data for all ionic liquids are obtained from dielectric measurements at ambient pressure except for the HMIM Cl, for which the transport quantities are also measured at different pressures as indicated

rearranging Eq. 2.7, it is clear that the observed universality of charge transport in ionic liquids as displayed in Fig. 2.9 is due to identical thermal activation of the charge transport rate and the viscosity, i.e., the product $\eta(T)\omega_c(T)/T$ exhibits negligible temperature and pressure dependence. This embodies the link between charge transport and structural relaxation in the ionic liquids studied.

Further insight into the correlation between charge transport and dynamic glass transition can be gained by comparison of viscosity obtained from dynamic mechanical spectroscopy (DMS) and the charge transport rate ω_c. Due to technical reasons, DMS only covers a spectral range spanning about 3–4 decades. This is about nine orders of magnitude less that the range accessible by broadband dielectric spectroscopy. To circumvent this difficulty and compare dielectric and DMS results over many decades, the structural relaxation rate ω_η can be approximated using Maxwell relation, $\omega_\eta = \frac{G_\infty}{\eta}$, assuming a temperature independent instantaneous shear modulus (typically 0.1 GPa) and position fluctuations (typically 0.2 nm). Based on Einstein–Smoluchowski, Stokes–Einstein and Maxwell relations one can easily show that $\omega_c = P\omega_\eta$, where $P = kT/\left(3\pi G_\infty a\lambda^2\right)$. Figure 2.10 demonstrates that $\omega_c \cong \omega_\eta$ over 6 decades and P is a constant of order one within experimental accuracy. These two rates can be compared more directly by making dielectric and DMS measurements at temperatures just above the calorimetric glass transition as shown Fig. 2.10. The rate ω_η obtained from the peak in G'' is observed to be in quantitative agreement with the charge transport rate ω_c determined from the dielectric spectra. It is therefore experimentally established that ω_c is ω_η in

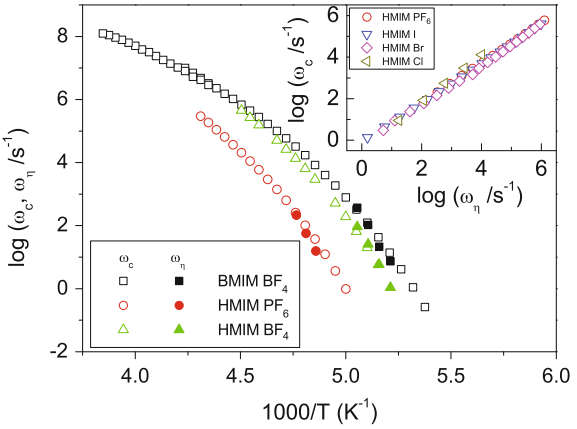

Fig. 2.10 The temperature dependence of the characteristic charge transport rate ω_c as well as the structural relaxation rate, $\omega_\eta\omega_\eta$, determined from dynamic mechanical spectroscopy (DMS) measurements for selected ionic liquids as shown. The two characteristic rates practically coincide within the spectral range measured. *Inset* The characteristic charge transport rate ω_c versus the structural relaxation rate, ω_η, determined from viscosity by applying the Maxwell relation given by $\omega_\eta = \frac{G_\infty}{\eta}$. Reprinted with permission from (*Acc. Chem. Res.*, 2012, 45 (4), pp. 525–532). Copyright (2012) American Chemical Society

glass-forming ionic liquids. The observed universality is thus understood based on Einstein's predictions as already discussed.

According to Eq. 2.6, the measured σ_0 is a product of the mobility and the effective number density of charge carriers contributing to ionic transport. It is essential to identify which of the two quantities gives the dc conductivity its characteristic VFT-type temperature dependence. In addition, it is helpful to find out whether one of the two quantities has greater influence on the ionic conductivity. For electronic conductors, *Hall Effect* measurements provide a means of disentangling the contributions of n and μ to the measured electrical conductivity, but the Hall voltages associated with ionic transport are at the nano-volt levels and are therefore too small to be determined with sufficient accuracy using state-of-the-art equipment. In addition, the validity of Hall measurements on ionic conductors is still in doubt [48].

Estimative determinations of the diffusion coefficients can be made by applying Eq. 2.6 and taking for the hopping length, values in the order of the Pauling diameter [49], i.e. $\lambda = 0.17$ nm and $\lambda = 0.19$ nm for [BMIM] [BF_4] and [MMIM] [Me_2PO_4], respectively. Independent results from PFG NMR together with the diffusion coefficients obtained from dielectric measurements are shown in Fig. 2.11. This simple method yields diffusion coefficients in agreement with those obtained by PFG NMR [22, 23]. Additionally, these experimentally determined diffusivities have been shown to coincide with those found from computations involving the Green–Kubo and Einstein relations as shown for [BMIM] [Br] in Fig. 2.12. These estimates make it possible to disentangle (using Eq. 2.6) the influence of n, the

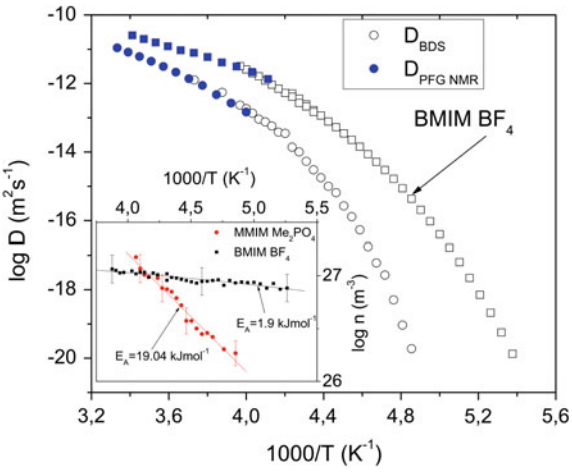

Fig. 2.11 Diffusion coefficient determined by the novel approach involving application of the Einstein–Smolukowski equation (using ω_c as hopping rate and with λ equal to the Pauling diameter of the ions as hopping length [49]), compared with the diffusion coefficient measured by PFG NMR (*blue colour*) for two ionic liquids: BMIM BF_4 and MMIM Me_2PO_4 [22, 23]. *Inset* Effective number of charge carriers as a function of inverse temperature (the respective activation energies are as indicated). The error bars are comparable to the size of the symbols, if not specified otherwise. Log is used to refer to logarithm to base 10

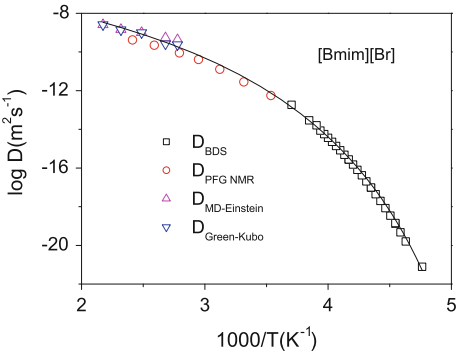

Fig. 2.12 Diffusion coefficients obtained from the dielectric spectra by application of the Einstein–Smoluchowski relation as well as those measured by PFG NMR for the ionic liquid [BMIM] [Br]. In addition, diffusion coefficients determined computationally by Einstein and Green-Kubo equations from quantum mechanical simulations are presented as well. Reprinted with permission from (*Acc. Chem. Res.*, 2012, 45 (4), pp. 525–532). Copyright (2012) American Chemical Society

effective number density, from that of the electrical mobility, μ. It is found that the VFT-type of thermal activation of the ionic conductivity originates exclusively from a similar dependence of the diffusion coefficient. In contrast, the effective number density of the ions exhibits Arrhenius type of temperature dependence (inset of Fig. 2.11). By extrapolating the effective number density to room temperature, one obtains 2.9×10^{27} m^{-3} for [BMIM] [BF_4], close to 3.4×10^{27} m^{-3}, which is the stoichiometric number of ions in the system. Therefore, around 85 % of the available charge carriers participate in ionic transport at room temperature. This result agrees with recent reports suggesting that only a fraction of the available charge carriers actually participate in the conduction process [12–14]. We have demonstrated that the approach to determine diffusion coefficient from dielectric spectra holds for other glass-forming systems as well [35]. Thus, this approach enables the determination of diffusion coefficient spanning many orders of magnitude by broadband dielectric spectroscopy.

2.3.2 *Elucidating the Correlation Between Characteristic Hopping Lengths and Molecular Volumes of Ionic Liquids*

There is a concerted effort aimed at understanding the physico-chemical properties of ionic liquids (ILs). In general, they exhibit a unique mix of interesting properties such as high conductivities, wide electrochemical windows, thermal stability, negligible vapour pressures, wide liquid ranges and low melting points, which makes them promising for use in power sources for electric vehicles, hybrid cars,

electronic and power storage devices [22, 23, 34, 50, 51]. It is estimated that it is possible to synthesize up to about 10^{18} different ILs based on the combinations of cations and anions available [20, 33]. Thus, it is imperative that more general relationships between the desirable properties such as high conductivities and the nature of anions and cations be established. Previous attempts to make quantitative predictions of the physical properties of ILs using quantitative structure–property relationships and molecular mechanics simulations have had some success [20]. The major drawbacks of these approaches include the need for large experimental datasets to derive correlations, time consuming computational methods or at least some experimental data from the IL under study. In this section, the hopping lengths characterizing charge transport are investigated with respect to ionic volumes determined by quantum chemical calculations.

Quantum chemical calculations of molecular volumes of the ionic liquids were carried out using MOPAC2009 [52]. Semi-empirical quantum chemical calculations have been performed using MOPAC2009 and the PM6 [53] Hamiltonian for geometry optimization. The COSMO technique was applied to account for solvent effects [54]. The typical value of the static dielectric permittivity for many imidazolium-based ILs is $\varepsilon_s = 15$, so this value was assumed in the calculations [15, 25]. Because the molecular diameter is strongly dependent on the conformation of the molecule various conformers were considered (e.g. 56 conformers for $[DMIM]^+$). Molecular volumes, V, were obtained by modelling the molecule as a series of intersecting spheres, whose radii are determined by the atom type (as implemented in MOPAC2009 [52] by the COSMO [54] solvation model). By taking the longest distance between two atoms and adding the van der Waals radii of the atoms, the maximum molecular diameters, D, were determined. The van der Waals radii reported by Bondi [55] were assumed for the calculation of the volume V as well as the diameter D. The ranges of molecular dimensions obtained are presented in Table 2.3. The technique described has been shown to reproduce the well-established ionic volumes of many common ions [56]. The values obtained in our studies are systematically lower than volumes determined from crystal structures but they exhibit the same trends [20]. The volumes corresponding to those of the crystal structures could only be reproduced by choosing different van der Waals radii.

Table 2.3 Range of molecular volumes, V, and maximum diameters, D, for different conformations of the ions constituting the ionic liquids

Ion	V/nm^3	D/pm
[MVIM]	0.1205–0.1208	966–1018
[PropMIM]	0.1492–0.1524	989–1131
[PVIM]	0.2601–0.2722	1084–1522
[OVIM]	0.1694–0.1738	1118–1905
[OMIM]	0.2483–0.2619	1030–1768
[DMIM]	0.2899–0.3139	1053–2021
$[(CF_3SO_2)_2N]$ (or $[NTf_2]$)	0.1693–0.1748	1000–1027

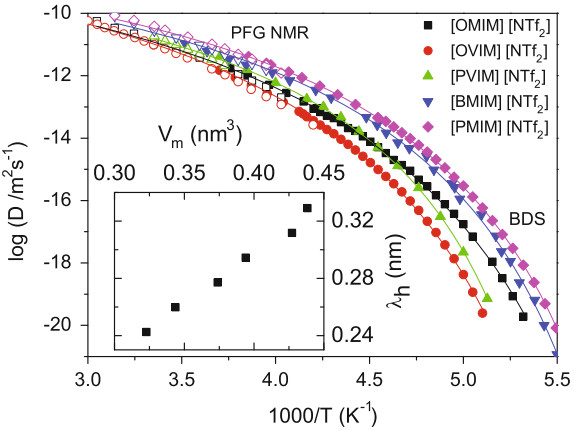

Fig. 2.13 Diffusion coefficients determined from broadband dielectric spectra (*filled symbols*) by applying the Einstein–Smoluchowski relation, using ω_c as the characteristic hopping rate for a series of ionic liquids based on the bis(trifluoromethylsulfonyl)imide anion as a function of inverse temperature. The diffusion coefficient measured by PFG NMR (*open symbols*) versus inverse temperature. *Inset* The mean hopping lengths λ_c (determined by the Einstein–Smoluchowski equation $(D = \lambda^2\omega_c/6)$ using ω_c obtained from BDS as the characteristic hopping rate and diffusion coefficient D measured by PFG NMR) versus the sum of molecular volumes of anions and cations from quantum chemical calculations for the different ionic liquids based on the same bis(trifluoromethylsulfonyl)imides anion. The calculation is carried out in the temperature ranges accessible to both techniques. Reprinted with permission from (*Acc. Chem. Res.*, 2012, 45 (4), pp. 525–532). Copyright (2012) American Chemical Society

Using a combination of PFG NMR and dielectric measurements, it is possible to calculate the characteristic hopping length λ_h, from diffusion coefficients and rates in the temperature range where the two techniques coincide. Based on Eq. 2.7, one can expect only a weak temperature dependence (if any) of λ_h given the universality of charge transport in ionic liquids as already discussed. The values of λ_h obtained are then used to determine diffusion coefficients from dielectric spectra of a series of ionic liquids as presented in Fig. 2.13. By that, it becomes possible to extend the range of diffusion coefficients measured by PFG NMR from about 4 to over 11 decades by employing dielectric spectroscopy. Consequently, electrical mobilities and effective number densities as well as their type of temperature dependence can be determined. The latter shows a weak Arrhenius-type dependence and is practically independent of the cation whereas the former exhibits a VFT—type behaviour and shows a pronounced dependence on the nature of the cation (especially at lower temperatures).

Central to the concept of diffusion within the linear response regime is the magnitude of the position fluctuations (also referred to as hopping lengths in the current chapter) λ of molecules in thermal equilibrium. Based on Einstein's [4] theory, the direct link to the diffusion coefficient was established. According to Eq. 2.7, molecular size has a direct influence on λ. The molecular volume of an IL

is a measure of its size and is more physically meaningful than the radius (or diameter). Based on quantum chemical calculations, it is possible to compute the molecular volumes of ionic liquids. Table 2.3 presents the results obtained for the series of ILs investigated. These are then compared with the values of λ obtained from diffusion measurements. It is observed that λ increases with the volume of the cation (see inset of Fig. 2.13). This can be interpreted in terms of the increase in the average distance between the ions for larger cations. One can expect that larger position fluctuations are only possible if adequate space is available. It has been shown that the knowledge of volumes of ILs can be used to successfully predict their physical properties [20].

Diffusion in dilute electrolytes comprised of multiple ionic species is often described by the Nernst–Hartley approach which neglects the contributions arising from ion–ion cross-correlation effects [57]. However, a general analytical expression of the diffusion coefficient for concentrated systems incorporating the contributions from the ion-correlation is yet to be found. It is therefore instructive to investigate the deviation from the predictions of the Nernst–Hartley equation and employ it as a means of quantifying the interaction of ionic species in ionic liquids. In two-component monovalent electrolytes, the effective diffusion coefficient within this framework is given by the Nernst-Hartley diffusion coefficient, D_{NH}, expressed as [57]:

$$D_{\mathrm{NH}} = \frac{2D_{\mathrm{A}}D_{\mathrm{C}}}{D_{\mathrm{A}} + D_{\mathrm{C}}} \tag{2.8}$$

where D_{A} and D_{C} denote the diffusion coefficients of the anion and cation, respectively. Based on Einstein–Smoluchowski relation, the effective characteristic diffusion (hopping) length, λ_{h} [in the timescale of the characteristic diffusion (charge transport) rate, ω_{c}, (described in Sect. 2.3.1)] can be defined with respect to the corresponding hopping lengths of the anions and cations given by λ_{A} and λ_{C}, respectively. If a single diffusion rate is further assumed, then the effective hopping length λ_{h} can be expressed as

$$\lambda_{\mathrm{h}} = \sqrt{\frac{2\lambda_{\mathrm{A}}^2\lambda_{\mathrm{C}}^2}{\lambda_{\mathrm{A}}^2 + \lambda_{\mathrm{C}}^2}} \tag{2.9}$$

As experimentally established in Sect. 2.3.1 of the current chapter, the diffusion rate, ω_{c} and the structural α-relaxation rate are identical. Given that the molecules experience mean displacements comparable to their diameters [58], it is worthwhile to estimate the average hopping lengths using Eq. 2.9 and diameters of anions as well as cations obtained from quantum chemical calculations. Based on the data in Table 2.3 as well as Eq. 2.9, this consideration yields effective hopping lengths of the order of 5 Å in contrast to the typical 2–3 Å determined experimentally for the

ionic liquids investigated. This disparity is indicative of the role of the cation–anion correlation in ionic liquids. Thus, the cross-correlation terms in ionic liquids are shown to be non-negligible. An adequate theory capable of describing diffusion coefficients in highly concentrated electrolytes such as ionic liquids is yet to be obtained. The Nernst–Hartley approach overestimates the diffusion coefficients because it does not consider the interaction between the anions and cations.

2.4 Conclusions

Because of the ease with which they can be supercooled, ionic liquids offer new opportunities to investigate long-standing problems regarding the nature of dynamic glass transition as well as its impact on charge transport. Despite the significant progress achieved so far from experimental and theoretical studies, no generally accepted quantitative theory of dynamic glass transition capable of reproducing all the experimentally observed features exists to date. In this chapter, we discuss recent studies on the interplay between charge transport and glassy dynamics in ionic liquids as investigated by a combination of several experimental techniques. Using Einstein–Smoluchowski relations, we suggest a simple approach to determine diffusion coefficients in a broad range spanning more than ten orders of magnitude from dielectric spectra of ionic liquids in quantitative agreement with independent pulsed-field gradient nuclear magnetic resonance measurements. This provides a new possibility to separately determine the electrical mobility and effective number density of charge carriers from the measured dc conductivity. The origin of the remarkable universality of charge transport in different classes of glass-forming ionic liquids is also unravelled.

Acknowledgments J. S. and T. C. acknowledge the National Science Foundation for financial support through the award number DMR-1508394. The authors gratefully acknowledge financial support from the Deutsche Forschungsgemeinschaft under the DFG SPP 1191 Priority Program on Ionic Liquids.

References

1. Chauvin Y (2006) Olefin metathesis: the early days (nobel lecture). Angew Chem Int Ed 45:3740–3747
2. Walden P (1914) Molecular weights and electrical conductivity of several fused salts. Acad Sci St. Petersburg 8:405–422
3. Plechkova NV, Seddon KR (2008) Applications of ionic liquids in the chemical industry. Chem Soc Rev 37(1):123–150
4. Einstein A (1905) Über die von der molekularkinetischen Theorie der Wärme geforderte Bewegung von in ruhenden Flüssigkeiten suspendierten Teilchen. Ann d Physik 17:549–560
5. Smoluchowski M (1906) Zur kinetischen Theorie der Brownschen Molekularbewegung und der Suspensionen. Ann d Physik 21:755–780

6. Smoluchowski, M (1906) On the mean path of molecules of gas and its relationship to the theory of diffusion. Bullet Intern Acad Cracovie: 202–213
7. Maxwell JC (1866) On the viscosity or internal friction of air and other gases. Philos Trans R Soc Lond 156:249–268
8. Maxwell JC (1867) On the dynamical theory of gases. Phil Trans Royal Soc London A 157:49–88
9. Langevin P (1908) Sur la théorie du mouvement brownien. C R Acad Sci (Paris) 146:530–533
10. Debye P, Hueckel E (1923) Zur Theorie der Elektrolyte I. Gefrierpunktserniedrigung und verwandte Erscheinungen. Physik. Z. 24:185–206
11. Xu W, Angell CA (2003) Solvent-free electrolytes with aqueous solution-like conductivities. Science 302(5644):422–425
12. Tokuda H, Hayamizu K, Ishii K, Susan H, Watanabe M (2005) Physicochemical properties and structures of room temperature ionic liquids. 2. Variation of alkyl chain length in imidazolium cation. J Phys Chem B 109(13):6103–6110
13. Tokuda H, Tsuzuki S, Susan H, Hayamizu K, Watanabe M (2006) How ionic are room-temperature ionic liquids? An indicator of the physicochemical properties. J Phys Chem B 110(39):19593–19600
14. Tokuda H, Ishii K, Susan H, Tsuzuki S, Hayamizu K, Watanabe M (2006) Physicochemical properties and structures of room-temperature ionic liquids. 3. Variation of cationic structures. J Phys Chem B 110(6):2833–2839
15. Weingaertner H (2006) The static dielectric constant of ionic liquids. Z Phys Chem 220:1395–1405
16. Ito N, Huang W, Richert R (2006) Dynamics of a supercooled ionic liquid studied by optical and dielectric spectroscopy. J Phys Chem B 110(9):4371–4377
17. Rivera A, Roessler EA (2006) Evidence of secondary relaxations in the dielectric spectra of ionic liquids. Phys Rev B 73(21):212201–212204
18. Ito N, Richert R (2007) Solvation dynamics and electric field relaxation in an imidazolium-pf6 ionic liquid: from room temperature to the glass transition. J Phys Chem B 111(18):5016–5022
19. Rivera A, Brodin A, Pugachev A, Roessler EA (2007) Orientational and translational dynamics in room temperature ionic liquids. J Chem Phys 126(11):114503–114507
20. Slattery JM, Daguenet C, Dyson PJ, Schubert TJS, Krossing I (2007) How to predict the physical properties of ionic liquids: a volume-based approach. Angew Chem Int Ed 46:5384–5388
21. Leys J, Wuebbenhorst M, Menon CP, Rajesh R, Thoen J, Glorieux C, Nockemann P, Thijs B, Binnemans K, Longuemart S (2008) Temperature dependence of the electrical conductivity of imidazolium ionic liquids. J Chem Phys 128(6):064509
22. Sangoro J, Iacob I, Serghei A, Naumov S, Galvosas P, Kaerger J, Wespe C, Bordusa F, Kremer F (2008) Charge transport and mass transport in imidazolium-based ionic liquids. Phys Rev E 77(5 Pt 1):051202
23. Sangoro J, Iacob I, Serghei A, Naumov S, Galvosas P, Kaerger J, Wespe C, Bordusa F, Stoppa A, Hunger J, Buchner R, Kremer F (2008) Electrical conductivity and translational diffusion in the 1-butyl-3-methylimidazolium tetrafluoroborate ionic liquid. J Chem Phys 128 (21):214509
24. Turton DA, Hunger J, Stoppa A, Hefter G, Thoman A, Walther M, Buchner R, Wynne K (2009) Dynamics of imidazolium ionic liquids from a combined dielectric relaxation and optical kerr effect study: evidence for mesoscopic aggregation. J Am Chem Soc 131 (31):11140–11146
25. Hunger J, Stoppa A, Schroedle S, Hefter G, Buchner R (2009) Temperature dependence of the dielectric properties and dynamics of ionic liquids. Chem Phys Chem 10(4):723–733
26. Sidebottom DL (2009) Colloquium: understanding ion motion in disordered solids from impedance spectroscopy scaling. Rev Mod Phys 81(3):999
27. Krause C, Sangoro JR, Iacob C, Kremer F (2010) Charge transport and dipolar relaxations in imidazolium-based ionic liquids. J Phys Chem B 114(1):382–386

28. Sangoro JR, Iacob C, Naumov S, Valiullin R, Rexhausen H, Hunger J, Buchner R, Strehmel V, Karger J, Kremer F (2011) Diffusion in ionic liquids: the interplay between molecular structure and dynamics. Soft Matter 7:1678–1681
29. Sangoro JR, Kremer F (2012) Charge transport and glassy dynamics in ionic liquids. Acc Chem Res 45(4):525–532
30. Hensel-Bielowka S, Wojnarowska Z, Dzida M, Zor ebski E, Zorebski M, Geppert-Rybczyńska M, Peppel T, Grzybowska K, Wang Y, Sokolov AP, Paluch M (2015) Heterogeneous nature of relaxation dynamics of room-temperature ionic liquids (emim)2[co(ncs)4] and (bmim)2[co (ncs)4]. J Phys Chem C 119(35):20363–20368
31. Paluch M, Wojnarowska Z, Goodrich P, Jacquemin J, Pionteck J, Hensel-Bielowka S (2015) Can the scaling behavior of electric conductivity be used to probe the self-organizational changes in solution with respect to the ionic liquid structure? The case of [c8mim][ntf2]. Soft Matter 11:6520–6526
32. Kremer F, Schoenhals A (eds) (2003) Broadband dielectric spectroscopy. Springer, Berlin
33. Katritzky AR, Jain R, Lomaka A, Petrukhin R, Karelson M, Visser AE, Rogers RD (2002) Correlation of the melting points of potential ionic liquids (imidazolium bromides and benzimidazolium bromides) using the codessa program. J Chem Inf Comput Sci 42:225–231
34. Sangoro JR, Iacob C, Serghei A, Friedrich C, Kremer F (2009) Universal scaling of charge transport in glass-forming ionic liquids. Phys Chem Chem Phys 11(6):913–916
35. Sangoro JP, Turky G, Abdel Rehim M, Iacob C, Naumov S, Ghoneim A, Kaerger J, Kremer F (2009) Charge transport and dipolar relaxations in hyperbranched polyamide amines. Macromolecules 42(5):1648–1651
36. Iacob C, Sangoro JR, Serghei A, Naumov S, Korth Y, Kaerger J, Friedrich C, Kremer F (2008) Charge transport and glassy dynamics in imidazole-based liquids. J Chem Phys 129 (23):234511
37. Dyre JC (1988) Unified formalism for excess current noise in random-walk models. Phys Rev B 37(17):10143–10149
38. Boettger H, Bryksin VV (1985) Hopping conduction in solids. Akademie-Verlag, Berlin
39. Riande E, Díaz-Calleja R (2004) Electrical properties of polymers. Marcel Dekker, New York
40. Boettcher CJF, Bordewijk P (1978) Theory of electric polarization (vol II). Elsevier Academic Press, Amsterdam
41. Krause C, Sangoro JR, Iacob C, Kremer F (2009, Oct) Charge transport and dipolar relaxations in imidazolium-based ionic liquids. J Phys Chem B 114(1):382–386. doi:10.1021/jp908519u
42. Angell CA (1985) Strong and fragile liquids. In: Ngai KL, Wright GB (eds) Relaxations in complex systems. U.S. GPO, Washington, DC
43. Angell CA (1995) Formation of glasses from liquids and biopolymers. Science 267 (5206):1924–1935
44. Martinez LM, Angell CA (2001) A thermodynamic connection to the fragility of glass-forming liquids. Nature 410(6829):663–667
45. Dyre JC (2006) Colloquium: the glass transition and elastic models of glass-forming liquids. Rev Mod Phys 78(3):953
46. Roling B, Martiny C, Murugavel S (2001) Ionic conduction in glass: new information on the interrelation between the "jonscher behavior" and the "nearly constant-loss behavior" from broadband conductivity spectra. Phys Rev Lett 87(8):085901
47. Kubo R (1986) Brownian motion and nonequilibrium statistical mechanics. Science 233 (4761):330–334
48. Bruce P (ed) (1995) Chemistry of solid state materials: solid state electrochemistry. Cambridge University Press
49. Pauling L (1960) The nature of the chemical bond, 3rd edn. Cornell University Press, Ithaca, New York
50. Wasserscheid P, Welton W (eds) (2002) Ionic liquids in synthesis. Wiley-VCH Verlag, Weinheim

51. Welton T (1999) Room-temperature ionic liquids. Solvents for synthesis and catalysis. Chem Rev 99(8):2071–2084
52. Stewart JJP (2009) MOPAC2009: the next generation quantum chemistry tool for property prediction. A molecular dynamics simulation software
53. Stewart JJP (2007) Optimization of parameters for semi-empirical methods V: modification of NDDO approximations and application to 70 elements. J Mol Mod 13:1173–1213
54. Klamt A, Schuermann G (1993) Cosmo: a new approach to dielectric screening in solvents with explicit expressions for the screening energy and its gradient. J Chem Soc Perkin Trans 2:799–805
55. Bondi A (1964) van der Waals volumes and radii. J Phys Chem 68(3):441–451
56. Marcus Y (1997) Ion properties. Marcel Dekker, New York
57. Turq T, Barthel J, Chemla M (1992) Lecture notes in chemistry (57): transport, relaxation, and kinetic processes in electrolyte solutions. Springer, Heidelberg
58. Larini L, Ottochian A, De Michele C, Leporini D (2008) Universal scaling between structural relaxation and vibrational dynamics in glass-forming liquids and polymers. Nat Phys 4(1):42–45

http://www.springer.com/978-3-319-32487-6

Dielectric Properties of Ionic Liquids
Paluch, M. (Ed.)
2016, X, 237 p. 116 illus., 58 illus. in color., Hardcover
ISBN: 978-3-319-32487-6